Pressure-Controlled Fabrication of Stibnite Nanorods by the Solvothermal Decomposition of a Simple Single-Source Precursor

Jian Yang,[†,‡] Jing-hui Zeng,[†] Shu-Hong Yu,*[,†] Li Yang,[‡] Yu-Hen Zhang,[‡] and Yi-Tai Qian*[,†,‡]

Department of Chemistry, and Structure Research Laboratory, University of Science and Technology of China, Hefei, Anhui 230026, People's Republic of China

Received January 13, 2000. Revised Manuscript Received July 7, 2000

A simple single-source precursor to stibnite (Sb_2S_3) synthesized from $SbCl_3$ and thiourea in methanol was characterized. The thermal decomposition of the precursor in polar solvents resulted in the formation of one-dimensional Sb_2S_3 nanocrystallites with the growth direction along the *c* axis. It is found that the as-prepared Sb_2S_3 nanorods are formed through the spontaneous connection of adjacent particles. The pressure in the solvothermal process plays an important role in the formation of the nanorods.

Introduction

Owing to its good photoconductivity, antimony trisulfide(stibnite) is regarded as a prospective material for solar energy.[1,2]Meanwhile, stibnite also belongs to the family of solid-state materials with potential applications in thermoelectric-cooling technologies.[3] Heavy-metal chalcogenides in glass are promising materials for use in optoelectronics and as optic fibers in the IR region.[4,5] Another important function of Sb_2S_3 is that it can be used as the starting material for the syntheses of sulfoantimonates of antimony and related compounds.[6] Schimek and co-workers took Sb_2S_3 as the reactant for a series of sulfoantimonates such as $M(NH_3)_6Cu_8Sb_3S_{13}$ (M = Mn, Fe, Ni).

Stibnite has been synthesized by various methods, such as vacuum evaporation,[7] chemical reaction methods,[8−10] and thermal decomposition.[11] Ghosh and Varma prepared amorphous and polycrystalline Sb_2S_3 films through vacuum evaporation.[7] However, this method often results in nonstoichiometry of the films owing to the differences in the vapor pressures of the reacting species.[5] In contrast, chemical reaction methods that do not involve sophisticated vacuum systems and heating apparatus have some advantages for the preparation of stibnite. Various sulfur ion sources, such as thioacetamide (TAM), sodium thiosulfate, or thiourea, and various complex agents, such as triethanolamine (TEA), ethylenediaminetetraacetic acid (EDTA), or tartartic acid, were used as the reactants in an aqueous bath.[10] Since most of the as-prepared Sb_2S_3 films were amorphous, they needed to be annealed at high temperature in air or in N_2 atmosphere to crystallize. Chocklingam prepared thick amorphous Sb_2S_3 films by precipitating $SbCl_3$ with ammonium sulfide.[8] To obtain the crystalline phase, the initial films were heated at around 600 °C in air. Similar reactions carried out in refluxing toluene for antimony oxides and chalcogenides have been reported by Parkin.[9] The thermal decompositions of some complexes, such as metal−ethylxanthate or antimony−tris(*N*,*N*′-disubtituted dithoicarbamate) were also employed to produce Sb_2S_3 powders.[11]

Currently, one-dimensional (1D) nanostructure materials have been the focus of recent scientific researches owing to their unusual properties and their potential applications for the development of nanodevices.[12,13] Therefore, the syntheses of semiconductor nanowires, nanorods, or fibers and the investigation of their prop-

* Corresponding author. E-mail: shyu@ustc.edu.cn.
† Department of Chemistry.
‡ Structure Research Laboratory.

(1) Nair, M. T. S.; Nair, K.; Garcia, V. M.; Pena, Y.; Arenas, O. L.; Garcia, J. C.; Gomez-Daza, O. *Proc. SPIE-Int. Soc. Opt. Eng.* **1997**, *3138*, 186.
(2) Savadogo, O.; Mondal, K. C. *Sol. Energy Mater. Sol. Cells* **1992**, *26*, 117.
(3) Smith, J. D. Arsenic, antimony, and bismuth. In *Comprehensive Inorganic Chemistry;* Pergamon Press: Oxford, 1973; Vol. 2, Chapter 21, p 547.
(4) (a) Baidakov, L. A. *NATO ASI Ser., Ser. 3* **1997**, *36, 171.* (b) Arivuoli, D.; Gnanam, F. D.; Ramasamy, P. *J. Mater. Sci. Lett.* **1988**, *7*, 711.
(5) Abrikosov, N. Kh.; Bankina, V. F.; Poretakaya, L. V.; Shelimova, L. E.; Skudnova, E. V. In *Semiconducting II−VI and V−VI Compounds;* Tybulewicz, A., Ed.; Plenum: New York, 1969; p 186.
(6) (a) Schimek, G. L.; W. Kolis, J.; Long, G. J. *Chem. Mater.* **1997**, *9 (12)*, 2776. (b) Stephan, H. O.; Kanatzidis, M. G. *Inorg. Chem.* **1997**, *36 (26)*, 6050.
(7) (a) Ghosh, C.; Varma, B. P. *Thin Solid Films* **1979**, *60*, 61. (b) Mahanty, S.; Merino, J. M.; Leon, M. *J. Vac. Sci. Technol., A* **1997**, *15 (6)*, 3060.
(8) Chocklingam, M. J.; Rao, M. J.; Rangarajan, N.; Suryanarayana, C. V. *J. Phys.* **1970**, *D3*, 1641.
(9) Carmalt, C. J.; Morrison, D. E.; Parkin, I. P. *Main Group Metal Chem.* **1999**, *22 (4)*, 263.
(10) (a) Desai, J. D.; Lokhande, C. D. *J. Non-Cryst. Solids* **1995**, *181*, 70. (b) Savadogo, O.; Mandal, K. C. *J. Electrochem. Soc.* **1992**, *139*, L16. (c) Rane, B. P.; Belle, M. I.; Hankare, P. P. *Bull. Electrochem.* **1993**, *9 (5−7)*, 237.
(11) (a) Lalia-Kantouri, M.; Manoussakis, G. E. *J. Therm. Anal.* **1984**, *29 (5)*, 1151. (b) Larionov, S. V.; Patrina, L. A.; Uskov, E. M. *Izv. Sib. Otd. Akad Nauk SSSR, Ser. Khim. Nauk* **1979**, *3*, 94.
(12) (a) Morales, A. M.; Lieber, C. M. *Science* **1998**, *279, 208*. (b) Han, W. Q.; Fan, S. S.; Li, Q. Q.; Hu, Y. D. *Science* **1997**, 277, 1287. (c) Alivisatos, A. P. *Science* **1996**, 271, 933.
(13) (a) Suenaga, K.; Colliex, C.; Demoncy, N.; Loiseau, A.; Pascard, H.; Willaime, F. *Science* **1997**, *278*, 653. (b) Dai, H.; Wong, E. W.; Lu, Y. Z.; Fan, S.; Liber, C. M. *Nature* **1995**, *375*, 769.

10.1021/cm000031t CCC: $19.00
Published on Web 09/08/2000

erties have aroused considerable interest.[12] Controlling the morphology and size of nanocrystallites is a new challenge to synthetic chemists and materials scientists.[14] Our group has successfully synthesized Bi_2S_3 nanowires via a solvothermal reaction.[15] But Sb_2S_3 powders prepared via the benzene-thermal reaction of anhydrous $SbCl_3$ with Na_2S_3 are composed of irregular nanoparticles with the average size about 150 nm.[16] To our best knowledge, one-dimensional stibnite has not been reported previously.

In this paper, an antimony−thiourea complex was produced by the reaction of $SbCl_3$ and thiourea in methanol and was found to be a good candidate for the fabrication of Sb_2S_3 nanorods via a solvothermal decomposition process. The spectroscopic properties of the complex were measured. The formation process of the nanorods in the solvothermal decomposition process was observed with XRD, EDAX, XPS, and TEM. It is interesting to note that the self-assembly of adjacent particles leads to the formation of Sb_2S_3 nanorods. The higher pressure of the environment is favorable for the formation of nanorods.

Experimental Section

Materials and Instruments. Anhydrous $SbCl_3$ (>99%), thiourea (>99%), and all solvents were procured commercially and were used without further purification. X-ray powder diffraction (XRD) patterns were obtained on a Japan Rigaku D/Max-γA rotation anode X-ray diffractometer equipped with the graphite-monochromatized Cu Kα radiation (λ = 1.541 78 Å), employing a scanning rate of 0.02 deg s^{-1} in the 2θ range from 10° to 70°. Transmission electron microscope (TEM) photographs, selected area electron diffraction (SAED) patterns, and energy-dispersive X-ray analysis (EDXA) were taken with a Hitachi model H-800 transmission electron microscope, using an accelerating voltage of 200 kV. The samples for these measurements were dispersed in absolute ethanol with an ultrasonic generator, and then the solutions were dropped onto copper grids coated with amorphous carbon films. X-ray photoelectron spectra (XPS) were recorded on a VEGSCALAB MKII X-ray photoelectron spectrometer, using nonmonochromatized Mg Kα radiation as the excitation source. IR spectra were measured on a Bruker Vector-22 FT-IR spectrometer from 4000 to 500 cm^{-1} at room temperature. The samples and KBr crystal were ground together, and the mixture was pressed into a flake for IR spectrum. ^{1}H NMR spectra were carried out on a FX-90Q spectrometer at the following frequency ^{1}H (60 MHz). Typical samples were prepared as 0.1−0.2 M solution of d_6-DMSO and were reported relative to TMS. UV−vis absorption spectra were obtained on a Shimadzu UV-2100 recording spectrophotometer scanning from 800 to 190 nm at room temperature with methanol as the reference. Diffuse reflection spectra of the samples were measured on a Shimadzu UV-240 recording spectrophotometer scanning from 850 to 500 nm at room temperature.

Preparation of a Simple Single-Source Precursor. First, thiourea (~60 mmol) was added to methanol (99.5%, 120 mL). Anhydrous $SbCl_3$ (~20 mmol) was added into that solution, after thiourea had been completely dissolved in methanol. The solution was stirred for approximately 30 min and then centrifuged to remove a small amount of undissolved material. The obtained yellow clear solution was condensed to 20 mL under the reduced pressure and allowed to stand overnight at room temperature. Yellow chrysanthemum-like powders that separated from the solution were filtrated, washed with absolute ethanol, and dried in a vacuum at 70 °C for 1 h. The obtained products were collected for characterization.

Preparation of Stibnite. The as-prepared precursor was redissolved in methanol, and the solution was placed into a Teflon-lined stainless autoclave to 80% of its capacity. After this the autoclave was maintained 2−12 h from 120 to 180 °C. Then the autoclave was cooled to room-temperature immediately. The as-prepared precipitates were filtrated, washed with distilled water, washed with absolute ethanol several times to remove byproducts, and dried in a vacuum at 70 °C for 1 h. The obtained powders were collected for characterization with XRD, TEM, SAED, EDXA, XPS, and the diffuse reflection spectrum.

Results and Discussion

The Single-Source Precursor. Complexes of antimony and thiourea have not attracted much attention. Most of the previous reports were by Russian scientists. For example, Vasil'ev and Gornostaeva studied the spectrophotometry of SbO^+−thiourea complexes in a $HClO_4$ or H_2SO_4 solution, respectively.[17] The solubility and the stability constants of antimony (Sb^{3+}) oxide in a $HClO_4$ solution containing thiourea were reported by Vasil'ev.[18] Gudimovich reported the isotherms of SbX_3−thiourea−H_2O (containing HCl) (X = F, Cl) systems at 25 °C.[19]

However, since anhydrous $SbCl_3$ hydrolyzes strongly in an aqueous solution, nonaqueous solvents are used to synthesize the complex. Meanwhile, owing to the good solubility of thiourea in it and its low boiling point, methanol is chosen as the solvent in this study. When anhydrous $SbCl_3$ was added to the methanol solution of thiourea, the solution immediately turned yellow, which implies that Sb^{3+}−thiourea complex is formed in the solution. The IR spectrum, UV−vis spectrum, and ^{1}H NMR spectrum confirmed this result. Chemical analysis also shows that the complex that separated from the solution contains Sb^{3+} and $CS(NH_2)_2$.[20]

In the IR spectrum of the Sb^{3+}−thiourea complex (Figure 1a), three characteristic absorption peaks at 3370, 3290, and 3184 cm^{-1} can be undoubtedly assigned to the $-NH_2$ stretching vibration. The $-NH_2$ bands did not shift to lower frequencies with regard to pure thiourea (Figure 1b), which indicates that a bond from the nitrogen to the metal is not present.[21] Meanwhile, the frequency of the C−N stretching vibration of the complex blue-shifted from 1474 cm^{-1} in pure thiourea to 1511 cm^{-1}, which approaches the value for a double bond. The blue shift of the C−N stretching vibration implies that thiourea uses the sulfur atom to coordinate with the metal ion in the complex.[22] The C═S stretching vibration of the complex at 1413 cm^{-1} was split into two peaks because of the formation of a metal−sulfur bond.[22]

(14) (a) Shiang, J. J.; Kadavanich, A. V.; Grubbs, R. K.; Alivisatos, A. P. *J. Phys. Chem.* **1995**, *99*, 17417. (b) Morris, R. F.; Weigel, S. *J. Chem. Soc. Rev.* **1997**, *26*, 309.

(15) Yu, S. H.; Shu, L.; Yang, J.; Han, Z. H.; Qian, Y. T.; Zhang, Y. H. *J. Mater. Res.* **1999**, *14 (11)*, *4157*.

(16) Yu, S. H.; Shu, L.; Wu, Y. S.; Qian, Y. T.; Xie, Y.; Yang, L. *Mater. Res. Bull.* **1998**, *33 (8)*, *1207*.

(17) (a) Vasil'ev, V. P.; Shorokhova, V. I.; Katrovtseva, A. V. *Zh. Neorg. Khim.* **1979**, *24 (10)*, 2652. (b) Gornostaeva, T. D.; Khmel′nitskays, O. D.; Shmargum, S. V.; Byval'tsev, V. Ya, Panchenko, A. F.; Lodeishckikov, V. V. *Zh. Neorg. Khim.* **1988**, *33* (1), 81.

(18) Vasil'ev, V. P.; Shorokhova, V. I.; Katrovtseva, A. V. *Zh. Neorg. Khim.* **1988**, *33 (3)*, 756.

(19) Godimovich, T. F.; Opalovskii, A. A.; Sokhranenko, G. P. *Zh. Prikl. Khim.* **1987**, *60 (10)*, 2188.

(20) *Handbook of Analytical Chemistry;* Chemical Industry Press: Beijing, China, 1997: Vol. 2, p 286; 1983: Vol. 3, p 563.

(21) Svatos, G. F.; Curran, C.; Quagliano, J. V. *J. Am. Chem. Soc.* **1955**, *77*, *6159*.

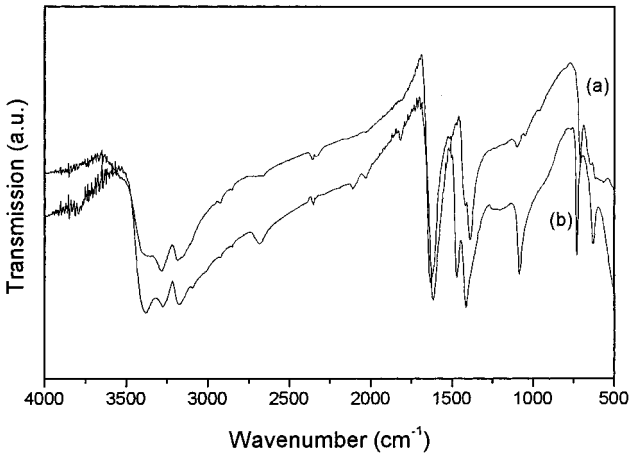

Figure 1. IR spectra of the as-prepared complex (a) and pure thiourea (b).

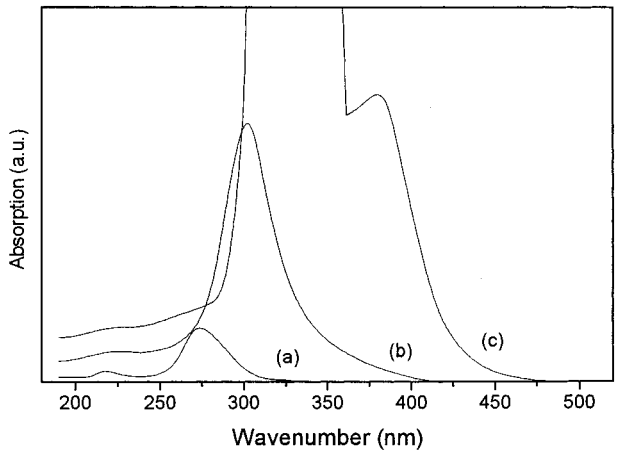

Figure 2. UV−vis absorption spectra of the complex in the different concentration solutions: (a) 6 mg/10 mL, (b) 30 mg/10 mL, (c) 150 mg/10 mL.

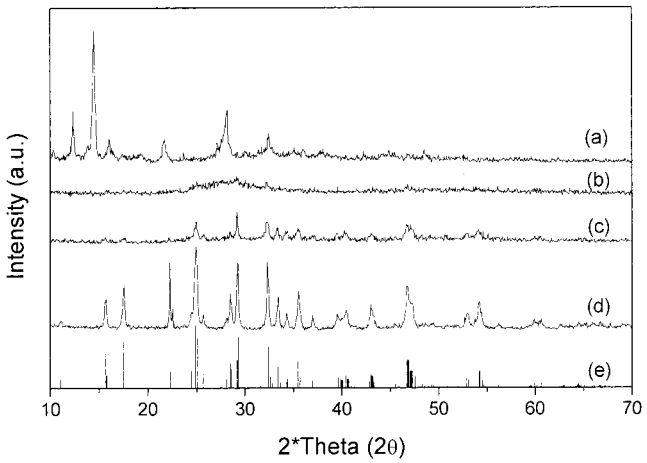

Figure 3. XRD patterns of the products obtained by the solvothermal decomposition after different times at 120 °C: (a) the precursor, (b) 2 h, (c) 3 h, (d) 6 h, (e) the standard pattern of stibnite.

Another very apparent difference in the IR spectrum between pure thiourea and the Sb^{3+}−thiourea complex appeared at approximately 1100 cm^{-1}. The strong absorption peak of pure thiourea at 1084 cm^{-1} was extremely weakened in the complex. In addition, another band associated with a C═S vibration of the complex was red-shifted from 729 cm^{-1} in pure thiourea to 709 cm^{-1}. The red shift can be attributed to the reduced double-bond character of the C═S bond owing to the sulfur bonding with the metal. The result is consistent with that obtained from the blue shift of the C−N stretching vibration. These characteristic shifts of absorption peaks demonstrate that thiourea uses the sulfur atom to coordinate with the metal ion in the complex.

The ^1H NMR spectrum presents one broad unresolved peak at 6.96 ppm that is shifted to high field with regard to pure thiourea.[23] It seems that the increase of electron density around the hydrogen atom is caused by the coordination of the ligand with the metal ion.

It is interesting to note that the absorption peaks of the complex shift to higher wavelength with increasing concentration of the complex. In the low-concentration solution of the complex (6 mg/10 mL), two absorption peaks at 221 and 266 nm were observed in the UV−vis spectrum, which is almost the same as that of the solution of thiourea.[24] This indicates that the interaction between Sb^{3+} and thiourea in the low-concentration solution is so weak that this interaction does not obviously affect the UV−vis spectrum of the ligand. Therefore, to clearly express the change in the UV−vis spectra due to the coordination, different concentration solutions of the complex were measured with the solution of thiourea as the reference. In this case, the band at 221 nm almost disappeared in the spectrum and the other was obviously weakened and slightly red-shifted to 270.5 nm (Figure 2a). If the solution concentration was increased to 30 mg/10 mL, the band previously at 270.5 nm moved to 302 nm (Figure 2b). When the solution concentration was further increased up to 150 mg/10 mL, there was a broad unresolved band from 301.5 to 359.0 nm and a shoulder at 383.5 nm in the spectrum (Figure 2c). It seems likely that these bands can be attributed to the charge-transfer transition from the ligand with chromophores to the metal ion at the center.[25] The appearance of a charge-transfer transition reveals that the interaction between the metal ion and thiourea is stronger at high-concentration solutions of the complex.

Formation of Sb_2S_3 Nanorods. To characterize the entire formation of stibnite nanorods, XRD, TEM, EDAX, and XPS were used to investigate the products obtained after different reaction times.

The XRD patterns of the products obtained after different reaction times show that the crystallinity of stibnite has been improved greatly with the prolonged reaction time. The XRD pattern of the as-prepared precursor indicates that it is of a polycrystalline nature. In this pattern (Figure 3a), no diffraction peaks corresponding to the starting materials were observed. When the precursor was treated in an autoclave for 2 h at 120 °C, amorphous stibnite was obtained, as is shown in

(22) Yamaguchi, A.; Penland, R. B.; Mizushima, S.; Lane, T. J.; Curran, C.; Quagliano, J. V. *J. Am. Chem. Soc.* **1958**, *80*, *527*. Swaminathan, K.; Irving, H. M. N. H. *J. Inorg. Nucl. Chem.* **1964**, *26*, *1291*.

(23) The Sadtler NMR Standard Spectra, 12880M.

(24) Zhou, M. C.; Yu, R. Q. *UV−Vis spectrophotometry;* Chemical Industry Press: Beijing, China, 1986; Chapter 2, p 83.

(25) Drago, R. *Physical Methods in Chemistry;* Saunders: Philadelphia, PA, 1997.

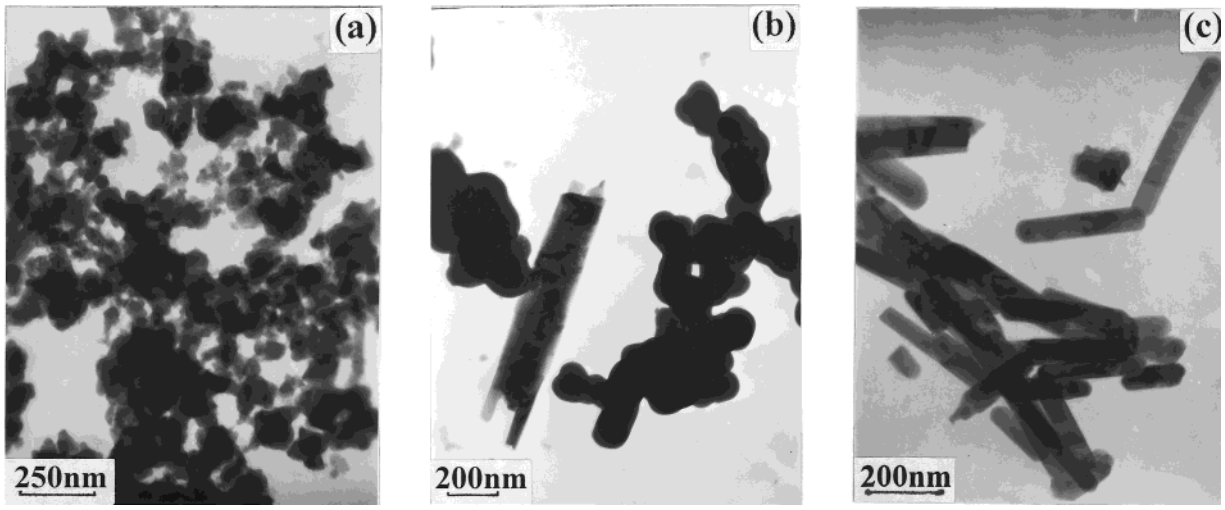

Figure 4. TEM photographs of the products obtained by the solvothermal decomposition of the precursor at 120 °C in an autoclave at different reaction times: (a) 2 h, (b) 3 h, (c) 6 h.

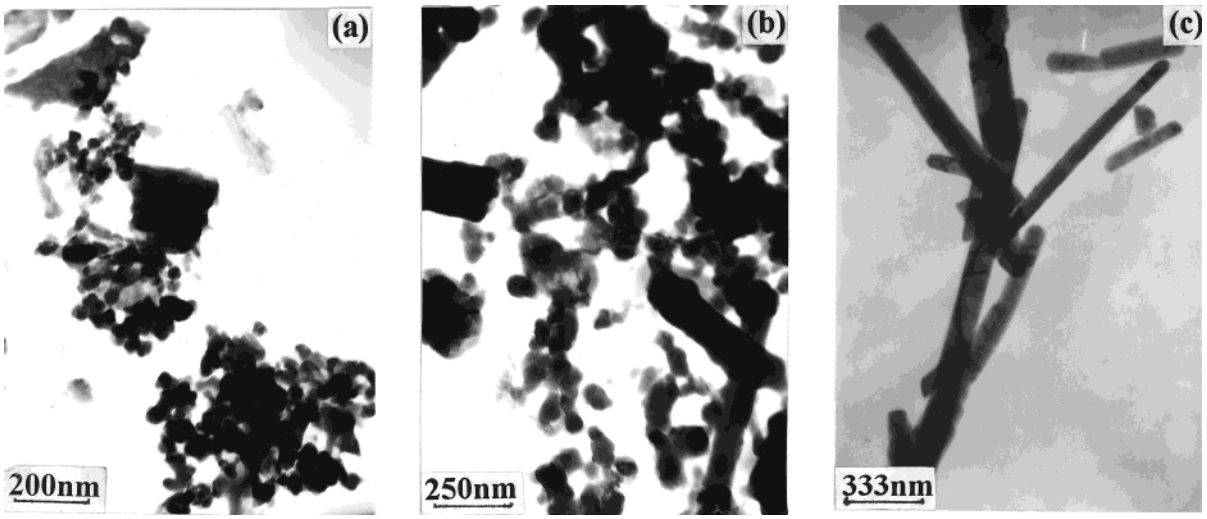

Figure 5. TEM photographs of the products obtained by (a) refluxing the methanol solution of the precursor for 6 h in a flask; (b) refluxing the methanol solution of the initial nanoparticles for 10 h in a flask; (c) maintaining the methanol solution of the initial nanoparticles at 120 °C for 10 h in an autoclave.

Figure 3b. EDAX and XPS were used to determine its composition. The result reveals that its composition is uniform and is close to the stoichiometry of stibnite. If the treatment time was prolonged to 3 h, the obtained violet-red stibnite was poorly crystallized, as is shown in Figure 3c. Until the treatment time reached 6 h, the obtained black-gray stibnite was not well crystallized. The crystalline products (Figure 3d) were identified as orthorhombic stibnite with cell constants $a = 11.228$ Å, $b = 11.329$ Å, $c = 3.844$ Å, which are close to the values in the literature.[26] The average crystal size calculated from the Scherer equation is 55 nm, which is close to the value measured from the TEM photographs.

TEM photographs corresponding to the products obtained after different reaction times are shown in Figure 4. When the reaction lasted for 2 h at 120 °C, the obtained Sb_2S_3 powders were composed of amorphous nanoparticles with an irregular shape and an average size at about 65 nm (Figure 4a). If the reaction time was prolonged to 3 h, some nanorods appeared in the poorly crystallized Sb_2S_3 powders (Figure 4b). After 6 h all the initial irregular particles transformed into well-crystallized nanorods (Figure 4c) with an average diameter of 60 nm that is close to the size of the initial amorphous nanoparticles. In this transformation process, many necklike connections were observed among the adjacent nanoparticles (Figure 4b). Meanwhile, in the head or edge of the nanorods just formed, there were many obvious bulges formed by different nanoparticles (Figure 5b). According to the above results, probably the initial adjacent nanoparticles self-assemble together to form the final Sb_2S_3 nanorods with the crystallinity improved, which does not resemble the formation process of CdS nanorods as observed in ethylenediamine.[27]

Since higher pressure is more favorable for the self-assembly of particles to form the necklike connections among them and a great number of connections among nanoparticles provide more opportunities for the formation of nanorods, this transformation is much faster in a closed system than that in an open system. This conclusion is confirmed by the experiments. When the

(26) JCPDS File, No. 6-0474.

(27) Yang, J.; Zeng, J. H.; Yu, S. H.; Yang, L.; Qian, Y. T. *Chem. Mater.*, in press.

Scheme 1. Pressure-Controlled Morphologies of Stibnite

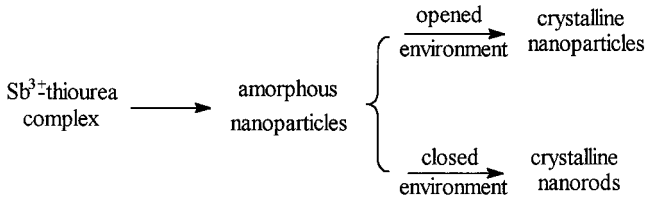

Scheme 2. Chain Structure of Stibnite

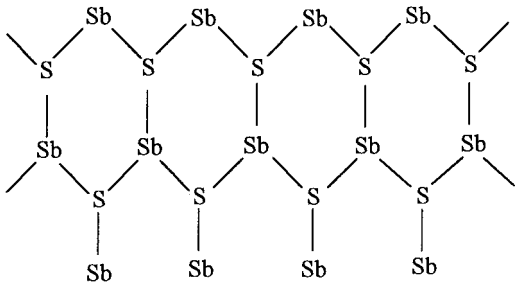

same system was refluxed for 6 h in an oil bath, the obtained products were still irregular nanoparticles, as is shown in Figure 5a. If the reflux time was prolonged to 10 h, some nanorods did appear in the products, although the majority of the latter remained as irregular particles (Figure 5b). The morphology transition of the products controlled by pressure is shown in Scheme 1.

The observed morphology of the as-prepared Sb_2S_3 powders is similar to that of Bi_2S_3 powders produced under sealed-tube pyrolysis of tris(benzylthiolato)bismuth ($Bi(SBn)_3$, Bn = $CH_2C_6H_5$) as reported by Boudjouk et al: [28]

$$2Bi(SBn)_3 \rightarrow Bi_2S_3 + 3Bn_2S \ (Bn = CH_2C_6H_5) \qquad (1)$$

It was found that the as-prepared Bi_2S_3 powders produced under the sealed environment were composed of spherical aggregates with acicular crystallites radiating from the center in a uniform size distribution. However, the Bi_2S_3 powders obtained under the flow pyrolysis consisted of aggregates of spherical particles.[28] In our route, the solvothermal synthesis was also conducted in a closed solution system, which is similar to the sealed-tube pyrolysis reaction of $Bi(SBn)_3$.

If the initial amorphous nanoparticles were taken out and were washed to remove the adsorbed reactants and byproducts, they still transformed to nanorods from the initial irregular nanoparticles as is shown in Figure 5c, when they were kept in a closed autoclave for 10 h at 120 °C. This implies that the transformation does not depend on the decomposition mechanism of the precursor. Since a similar phenomenon is also observed in other materials with the same structure as Bi_2S_3, the unusual chain structure of Sb_2S_3 (Scheme 2) probably plays a critical role in this transformation process.[29]

Since the nanorods can be produced in many polar solvents such as pyridine, this formation process of Sb_2S_3 nanorods does not depend on the solvent. However, the differences in the width and the length of the

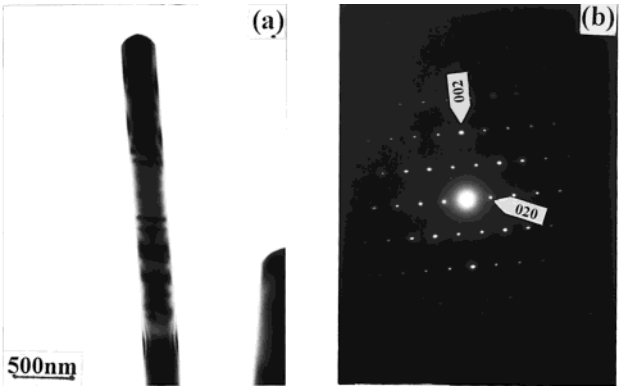

Figure 6. TEM photograph (a) and SAED pattern (b) of a typical Sb_2S_3 nanorod.

Sb_2S_3 nanowires synthesized from different solvents are related to the different physicochemical properties of the solvent. Solvent physicochemical properties such as polarity, viscosity, and softness will strongly influence the solubility and the transport behavior of the precursor.[30] In addition, the solvent acts as both the reaction medium and the dispersion medium so that it will greatly influence the nucleation and growth of the particles in the solvothermal process.

Characterization of Sb_2S_3 Nanorods. A typical Sb_2S_3 nanorod of 5 μm in length and 100 nm in width synthesized in methanol at 180 °C for 12 h is shown in Figure 6. Its SAED pattern shows that it is a well-developed single crystal with its growth direction along the *c* axis. It is apparent that there are many fine structures in the as-prepared Sb_2S_3 nanorods. Some short striations nearly perpendicular to the growth direction can often be observed in the products. It is believed that stacking faults are responsible for this.[31]

XPS was carried out to identify the composition. The typical survey spectrum of Sb_2S_3 is shown in Figure 7a, which reveals the presence of Sb, S, and contaminated C on the nanorod surface. High-resolution spectra were taken in the Sb and S regions of the products as shown in Figure 7b,c. Since the position of the Sb 3d5 binding energy is superposed with that of the O 2p binding energy, the Sb 4d binding energy was taken for characterization. The two strong peaks at 33.70 and 160.95 eV correspond to the Sb 4d and S 2p binding energies, respectively, which coincide with reports in the literature.[2] There were no peaks due to the elements or oxides in the XPS spectra. This can be attributed to the fact that the nonaqueous solvent effectively retarded the hydrolysis of the antimony ion. There was no evidence of shake-up peaks, which are photoemission peaks from species ionized prior to the observed photoemission process and generally occur at several electronvolts higher than the binding energy of the main peaks in the spectra. EDAX was used to determine the composition of these nanorods. The results show the compositions of these nanorods are uniform and the element ratio of Sb:S is 36.06:63.94 in agreement with the expected values.

The study of the optical properties of the materials provides a simple and effective method to explain some

(28) Boudjouk, P.; Remington, M. P.; Grier, D. G. Jr.; Jarabek, B. R.; McCarthy, G. J. *Inorg. Chem.* **1998**, *37*, *3538.*

(29) Wells, A. F. In *Inorganic Structure Chemistry;* New York, 1977*;* Chapter 20, p 907.

(30) Sheldrick, W. S.; Wachhold, M. *Angew. Chem., Int. Ed. Engl.* **1997**, *36*, 206.

(31) Trentler, T. J.; Hickman, J. M.; Goek, S. C.; Viano, A. M.; Gibbons, P. C.; Buhro, W. E. *Science* **1995**, *270*, *1791.*

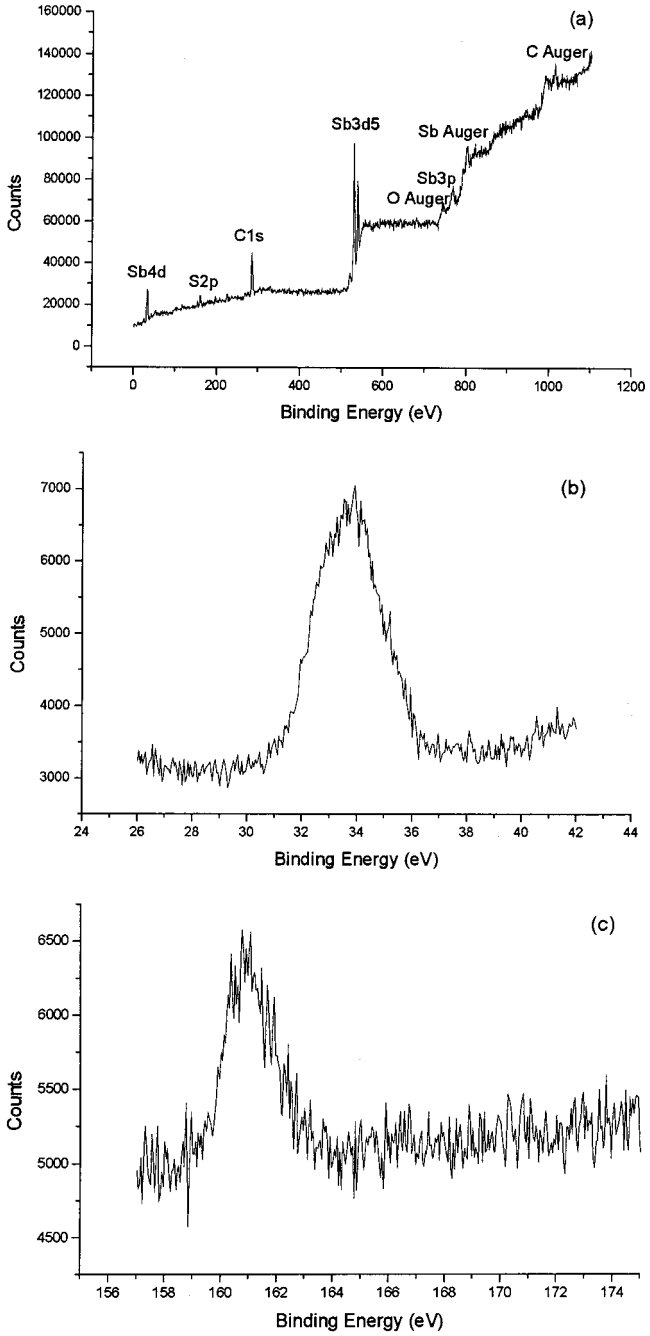

Figure 7. XPS spectra of Sb_2S_3 nanorods: (a) typical XPS survey spectrum of Sb_2S_3 nanorods, (b) close-up surveys for Sb 4d core, (c) close-up surveys for S 2p core.

features concerning the band structure. The diffuse reflectance spectra of the nanorods were measured at room temperature as is shown in Figure 8. In the spectrum of the crystalline nanorods, the diffuse reflectance sharply descends from 850 nm. The value of the band gap is determined by the intersection point of the

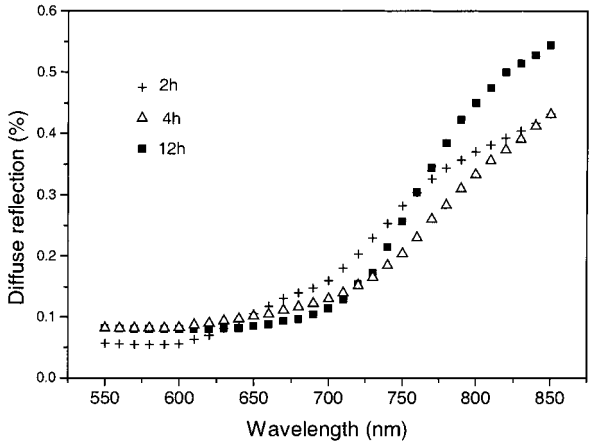

Figure 8. Diffuse reflection spectrum of the products at different times.

tangent of the absorption edge with the extended line of the diffuse reflectance at lower wavelength. The band gap of the crystalline products is about 1.75 eV, which is smaller than the band gap of the amorphous product at 1.87 eV. The value of the band gap of the stibnite nanorods is close to the bulk value reported by Savadogo.[1] But it is interesting to note that the band gap of this material decreases with the amorphous−crystalline transition of the products. A similar decrease in band gaps has also been observed previously in the same materials and other chalcogenides.[2,7] Manhanty found that this could be attributed to the higher degree of crystallinity and the increase in the grain size due to the amorphous−crystalline transition.[7b]

Conclusion

A novel solvothermal decomposition process has been successfully developed to fabricate Sb_2S_3 nanowires with an antimony−thiourea complex as the precursor. Details of the synthesis and spectroscopic characterization of the precursor were reported. The band gap of stibnite decreases during the amorphous−crystalline transition of the stibnite. Meanwhile, it is found that the as-prepared Sb_2S_3 nanorods with their growth direction along the *c* axis are formed by the spontaneous self-assembly of initial nanoparticles. The pressure of environment has a great influence on the transformation process.

Acknowledgment. This research is supported by the National Natural Science Research, Anhui Provincial Foundation of Natural Science Research, and the National Climbing Program. We gratefully thank Prof. G. E. Zhou for manipulating the X-ray diffractometer.

CM000031T